THE JOURNAL OF PHYSICAL CHEMISTRY Letters

Letter

pubs.acs.org/JPCL

Pronounced, Reversible, and in Situ Modification of the Electronic Structure of Graphene Oxide via Buckling below 160 K

Adrian Hunt,*[,†,§] Eamon McDermott,[†,∥] Ernst Z. Kurmaev,[‡] and Alexander Moewes*[,†]

[†]Department of Physics and Engineering Physics, University of Saskatchewan, 116 Science Place, Saskatoon, Saskatchewan S7N 5E2, Canada

[‡]Ural Federal University, 19 Mira Street, Yekaterinburg, Russia 620002

Supporting Information

ABSTRACT: We have shown that the electronic structure of graphene oxide is strongly, but reversibly, affected by temperature. Below 160 K, graphene oxide is much more completely oxidized, removing any last remaining π-conjugated network. Through DFT simulations, we have shown that this is due to buckling-induced oxidation. As temperature is reduced, the lightly oxidized, graphene-like zones attempt to expand due to a negative thermal expansion coefficient (TEC), but the heavily oxidized zones, with a TEC that is near zero, prevent this from happening. This contributes to localized buckling. The deformed regions oxidize much more readily, and the 1,2-epoxide groups form a new type of functional group never before seen: a triply bonded oxygen, bonded at the 1,3,5 sites of the hexagonal carbon rings. We have called this group TB-epoxide. Stable only under buckling, the TB-epoxide groups revert back to 1,2-epoxides once the lattice relaxes to a flatter profile. We have shown that one can alter the electronic structure of graphene oxide to induce temporary, but more complete, oxidation via strain.

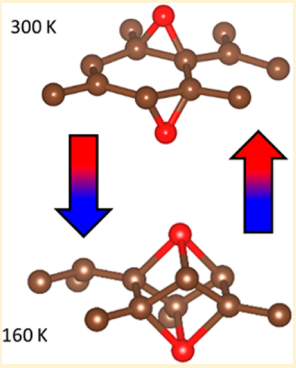

Graphene is a stable two-dimensional crystal, made of carbon atoms arranged in a hexagonal structure.[1] Research on graphene has been frenetic, but it is not hard to understand the interest this material commands. Pristine graphene is a zero band gap semiconductor, and the charge carriers near the Fermi level are massless Dirac Fermions, which give graphene unprecedented electronic properties.[2] Graphene, and its derivatives such as graphene oxide, have been implemented in a wide-ranging number of electronic and optoelectronic applications.[3−5] Graphene also has superior mechanical properties, and as such has also been effectively used in composite materials.[6,7] Although graphene possesses many amazing qualities, it does not have a band gap, which means that pristine graphene is inappropriate in many applications that require a true semiconductor. Significant oxidation of graphene does open a semiconducting band gap, but unfortunately destroys the π-conjugated network that grants graphene its unique characteristics, even after chemical reduction to remove some of the functional groups.[8] Thus, one must either repair the damage to the carbon basal plane,[9] or modify the electronic structure of graphene without damaging it, such as by noncovalent functionalization.[10] At least, this is the prevailing wisdom. As we will show, the electronic structure of lightly oxidized graphene can be changed at will simply by changing the temperature, via reversible, buckling-induced oxidation.

The literature has indeed shown that the electronic structure of graphene oxide (GO) is a complex function of temperature. The low temperature range, namely below 0 °C, has been shown to exhibit or induce some interesting phenomena. Su et al. have found that the Young's modulus of graphene oxide paper varies with temperature with a hysteresis curve below 25 °C.[11] Huang et al. found that the conductivity of multilayered graphene oxide was strongly dependent on temperature. Their samples transition between semiconducting and insulating behavior at several different temperatures,[12] a phenomenon that they attributed to interactions with water. Below 10 °C, the sample is an insulator. Hauptmann et al., however, showed no such change in the conduction behavior of their samples. Over the range that Hauptmann et al. examined, the change in conductivity as a function of temperature does not deviate from that of a material that obeys a variable range hopping model of conduction.[13] Although it is clear that GO does undergo some change at low temperatures, an understanding of what occurs remains elusive; there is only scant information available, and the few studies that have been published paint a contradictory picture of what actually occurs when GO is cooled.

We explain here why the electronic structure of GO changes at low temperatures. To this end, we have performed X-ray absorption near edge spectroscopy (XANES) experiments upon four multilayered GO samples and analyzed the results by comparing the spectra to density functional theory (DFT) simulations. Each of the four samples was prepared differently, and they are labeled GOa, GOb, GOc, and GOd. Important points of information concerning the preparation of these four samples are detailed in Table 1. The preparation methodology used to make our samples of multilayered graphene oxide paper is discussed elsewhere.[14,15] All samples were derived from the

Received: May 4, 2015
Accepted: July 17, 2015
Published: July 17, 2015

DOI: 10.1021/acs.jpclett.5b00921
J. Phys. Chem. Lett. 2015, 6, 3163−3169

Table 1. Details Concerning the Preparation of the Four GO Samples

sample	method of manufacture
GOa	GO paper from water filtration
GOb	GO paper intercalated with hexylamine and dried
GOc	GO water suspension; water was substituted with DMSO and filtered
GOd	GO water suspension; water was substituted with DMSO and heated in solution, then filtered

same GO base material, which was made via the modified Hummers method and subsequent water filtration. However, each has a different interlayer chemistry, which was why we chose them for this study.

We have probed the samples of GO using C 1*s* and O 1*s* XANES, which are shown in Figure 1. The C 1*s* and O 1*s* XANES spectra represent the core hole-perturbed unoccupied partial density of states (pDOS) near to the C and O sites, respectively. All XANES spectra were measured at the Spherical Grating Monochromator (SGM) beamline at the Canadian Light Source.[16] The XANES were measured in total fluorescence yield (TFY) mode. More details can be found in the Experimental Section.

The samples were first cooled to 120 K under ultrahigh vacuum (UHV) conditions, and the O 1*s* and C 1*s* XANES spectra were measured. The temperatures of the samples were then increased in 40 K increments to 160 K, 200 K, and finally 240 K, with spectra recorded at each step. To mitigate radiation damage effects, all spectra were measured in fast scanning mode. This mode collects data constantly while rapidly moving through the energy range of the scan, rather than the stop-and-record method that is far more typical of XANES experimentation apparatuses. Each XANES spectrum shown in Figure 1 was measured in 20 s. Additionally, each spectrum was measured while irradiating a new spot on the sample in question. This was done not only to keep radiation damage to a minimum, but also to keep localized heat loading from the X-rays from warming the illuminated area too much in relation to the bulk temperature of the sample. Once the samples had returned to room temperature, still within UHV, the samples were cooled to 240 K, and back down to 120 K in 40 K steps. On the cooling cycle, we measured only the C 1*s* spectra as we were primarily interested in the hysteresis of the C partial density of states (pDOS).

There are two observations that are immediately clear from the C 1*s* data in Figure 1: (1) the unoccupied C pDOS changes significantly, and (2) there is a clear hysteresis effect with temperature. Concerning the hysteresis, the samples all seem to retain high temperature (HT) characteristics until reaching some threshold transition temperature between 160 and 120 K. Upon warming, the electronic structures of the samples retain much low temperature (LT) character until they have been fully warmed. Between the two extremes, a metastable state seems to exist where characteristics of both HT and LT states are present, although the dominant member of the mix depends on which temperature extreme has been most recently experienced by the sample.

Concerning the electronic structure of the samples, there are two significant changes in the C unoccupied pDOS as one cools the sample. First, there is significant suppression of the residual C 1s → π^* resonance at 285.2 eV (feature *b* in Figure 1), with a concomitant enhancement of the main functional group resonances around 288.4 eV (feature *c*). This is true for all samples. GOd, however, uniquely possesses feature *d*. At 291.5 eV, this is the C 1s → σ^* resonance of sp^2 bonded carbon, which means that the HT state of GOd sees a stronger

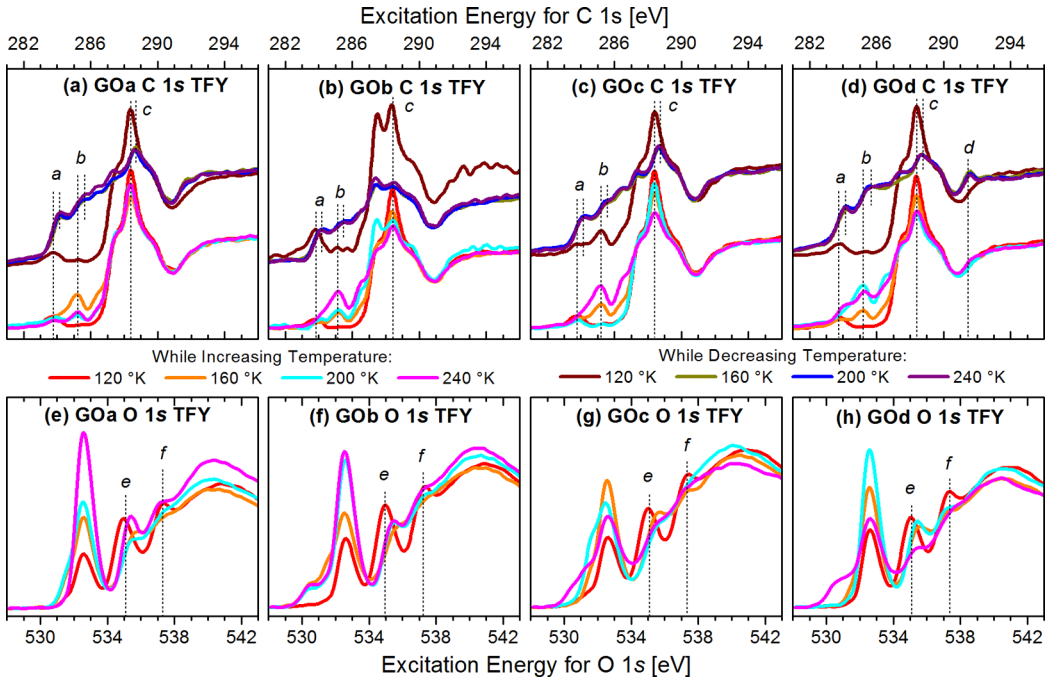

Figure 1. C 1*s* and O 1*s* XANES spectra of four samples of GO, measured at various temperatures. The spectra in the top row are the C 1*s* spectra, while the bottom row holds the O 1*s* spectra. All lighter-colored spectra (red, orange, cyan, magenta) were measured after first cooling the samples to 120 K, then warming sequentially to 240 K. All darker-colored spectra (dark red, dark yellow, dark blue, and purple) were measured by cooling the samples from room temperature to 120 K. Only C 1*s* spectra were measured on the cooling cycle. All C and O 1*s* XANES spectra were measured with the incoming radiation striking at an angle of incidence of 30° from the normal of the sample.

DOI: 10.1021/acs.jpclett.5b00921
J. Phys. Chem. Lett. 2015, 6, 3163−3169

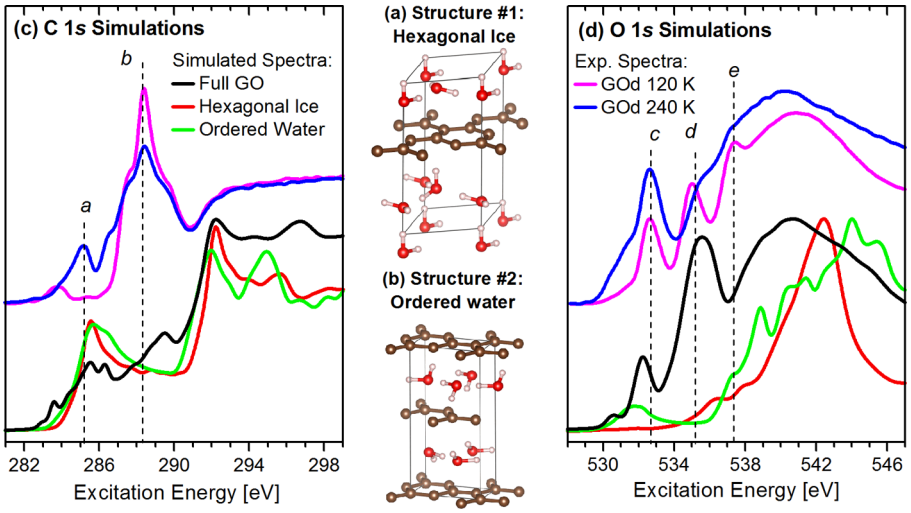

Figure 2. DFT simulations of the electronic structure of graphene interacting with different crystalline forms of water. Experimental C 1*s* and O 1*s* XANES spectra from GOd are included for comparison. Panels a and b show the structures. Panel c displays the comparison of the calculated C 1*s* XANES to the experimental XANES; panel d does likewise, but for the O 1*s* edge. The Full GO simulation has been presented previously in ref 30. Assignment of the peaks is discussed in the Supporting Information, and displayed in Figure S3.

sp^2 network than the other samples. This is fitting considering that GOd was the only sample to be heated after treatment, which would help to rebuild the π-conjugated network (see Table 1). The fact that the cooling effect suppresses both of the residual π^* and σ^* states is significant, as it would seem that it targets the residual sp^2 bonded carbon. There is also a general shift in energy for the π^* and functional group spectral features. With the exception of GOb, all of the easily resolvable resonances are red-shifted by 0.3 to 0.4 eV at LT as compared to their HT counterparts, except for the π^* feature. There are two exceptions to this rule. Feature *c* in the GOb spectrum does not shift, even as *a* and *b* do. However, it is also clear that the functional group chemistry of this sample is significantly different given the feature at 287.5 eV that is not present to any great degree in the other samples. Given that GOb is the only sample intercalated with hexylamine, it would seem that the initial cooling cycle permanently changed how hexylamine interacts with the host GO. The nature of this interaction is unknown.

The suppression of the π^* and σ^* states with a simultaneous enhancement of functional group states, particularly at 288.4 eV, suggests that the residual carbon sp^2 network is being functionalized.[17] Furthermore, the functionalization seems to be reversible. How is this possible? The first clue to understanding this phenomenon may be seen in the O 1*s* spectra for the samples. Although there are some minor differences between the spectra from the four samples, one trend holds true: In all cases, feature *e* at 535.1 eV, and feature *f* at 537.3 eV, are very prominent at 120 K and fade as one approaches room temperature. The speed of the decay of these features as a function of temperature depends upon the sample, but it occurs in the spectra of all samples.

Recalling that Huang et al. attributed to water the changes in conductivity of GO that they witnessed, let us consider the possible role of water. Indeed, water is an integral part of the chemistry of GO. GO has been shown to be highly permeable to water.[18,19] When heated, the presence of water has been shown to catalyze the decomposition of graphene into CO_2.[20,21] When multilayered GO is stored at room temperature, the interplanar water content increases over time as epoxide and hydroxyl groups both react with chemisorbed hydrogen.[22] Features *e* and *f* at LT are distinctive, and they match similarly sharp features seen in the O 1*s* XANES spectra of amorphous solid water.[23,24] Theoretical simulations of water also show strong features at the appropriate energies, but only when broken hydrogen bonds (specifically with dangling hydrogens) are present.[25]

Thus, previous work on amorphous solid water shows many spectroscopic similarities to the O 1*s* data in Figure 1. Other research into the interaction between water and organic systems has shown that, in the presence of organic materials with a mosaic of hydrophobic and hydrophilic zones like GO, water can form exotic structures.[26] In particular, the glass transition of water is below 160 K, which is the temperature range in which we see the dramatic change in electronic structure.[27] These reports apply here because GO synthesized with the modified Hummers method has significant amounts of intercalated water that is a residue from the initial synthesis process. Given that the electronic structure change seems to impact the residual sp^2 domains the strongest, we have attempted to simulate the change in electronic structure in GO at low temperatures by introducing ice between layers of graphene. The electronic structure simulations were performed using WIEN2k, a full-potential ab initio DFT code that uses linearly augmented plane wave (LAPW) formalism to describe the noncore states.[28] To try to account for dispersion forces, we used the Becke–Johnson (BJ) exchange-correlation potential implemented in WIEN2k.[29]

Our criterion for evaluating the success of a simulation was straightforward: Given that it is the residual π-conjugated states that are most affected as one cools the samples, the candidate structure must modify the graphene and/or lightly oxidized graphene unoccupied pDOS in such a way as to explain the changes in spectral shape. Our attempts to simulate the interaction between graphene and water are shown in Figure 2. For reference, we have included the C 1*s* and O 1*s* XANES spectra of GOd, measured at 120 and 240 K, as well as the composite simulated spectra GO that we calculated in previously published work, which includes epoxides, hydroxyls, and water.[30] When attempting to quantify the effect that

DOI: 10.1021/acs.jpclett.5b00921
J. Phys. Chem. Lett. 2015, 6, 3163−3169

amorphous solid water may have upon the graphene DOS, we simulated many different structures with water/graphene or water/oxidized graphene. The two that we chose to display in Figure 2 are (1) hexagonal ice (HI), and (2) ordered water (OW); the results of the electronic structure simulations of these two structures, as well as images of the crystal structures themselves, are presented. The HI and OW structures both incorporated sheets of graphene, rather than graphene oxide. The images of the units cells were prepared using VESTA.[31] The HI structure is similar to the optimized structure of Boukhvalov et al. in ref 19.

These two structures were chosen because, despite their very different physical structures, they come to the same result that we found to be typical of all of the simulations of graphene/water structures: amorphous solid water does not induce a change in the π^*-symmetry states of graphene. On the C 1*s* edge, neither structure reduces the π^* feature at 285.2 eV (peak *a*), nor shows any structure at peak *b*. On the O 1*s* edge, none of the three peaks that show strong change (peaks *c*, *d*, and *e*) are represented at all by the water/graphene structures. This result does not change even with light oxidation; any changes to the C pDOS of the graphene sheets is entirely due to the functional group. The structures, in CIF format, are available in the Supporting Information.

Water is thus not responsible for the observed electronic structure changes, at least not directly through noncovalent functionalization. However, there is another change that GO undergoes at low temperatures that water, in amorphous solid water form, may affect: physical changes via thermally induced buckling. As it turns out, graphene has a negative thermal expansion coefficient (TEC), down to 100 K.[32,33] GO, on the other hand, has an intrinsic TEC that is near zero, but when GO is in a water-rich environment, the system has an overall negative TEC as well.[34] However, within an individual GO flake, there will be a struggle between the highly oxidized zones, which will not change much as the temperature drops, and the lightly oxidized zones, where the TEC will be closer to that of graphene and thus will want to expand. Given that the highly oxidized zones will be in the majority, the graphene-like areas will not be able to properly expand, and will instead buckle under the strain.

It is in this buckled, lightly oxidized zone that a new functional group is formed, shown in Figure 3. Likely originating with the epoxide groups that populate such zones,[8] oxygen sites with three bonds form, such that the oxygen is bonded to the 1,3,5 carbon sites around the highly distorted aromatic rings. Given that epoxides are supposed to bond to graphene in pairs—one on each site of the graphene lattice—then another oxygen on the other side of the graphene sheet forms bonds with the 2,4,6 carbon sites. Because the O site has three bonds, we call this functional group triple-bonded epoxide (TB-epoxide). Details concerning the process by which the TB-epoxide structure was optimized and simulated, as well as structural characteristics such as bond lengths, are including in the Supporting Information, particularly Figure S1.

To the best of our knowledge, this functional group has not been identified before. However, this may simply be due to the peculiar way it bonds to the graphene lattice. The widely accepted functional groups that bond to graphene, such as epoxides, hydroxyls, carboxyls, and ketones, can all bond to the outer edges of cyclic organic structures, such as benzene. TB-epoxide, however, cannot. An oxygen atom can form a TB-epoxide group only on the face of an aromatic ring, and as such,

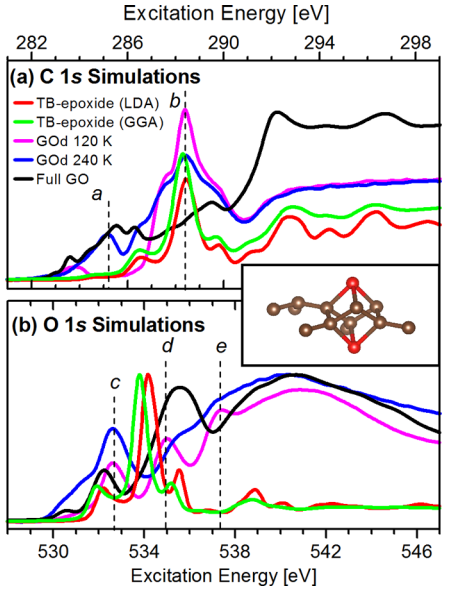

Figure 3. Simulations of the C 1*s* XANES, in panel a, and O 1*s* XANES, in panel b, that one would expect to measure from the new functional group, TB-epoxide, for both the LDA- and GGA-optimized strctures. The simulations are spin-polarized, but the difference between the spin-up and spin-down projections were negligible, thus only the spin-up projections are shown. The inset shows the functional group. The formation of this functional group is not spontaneous, but rather requires the graphene lattice to become highly buckled via some external means.

can only form on molecules with a two-dimensional lattice that is sufficiently large as to allow for the buckling that TB-epoxide requires with breaking the molecule. That leaves graphene, and possibly carbon nanotubes of a sufficiently large radius, as the only viable candidates for observing this unique functional group.

The electronic structure simulations, as well as an image of this new functional species, are shown in Figure 3; a larger image of the functional group is available in Figure S1 in the Supporting Information. It should be noted here that the energy axis of these calculations, much like the graphene/ice calculations shown earlier, were shifted by an amount identical to the simulation of a known system. In the case of the C 1*s* simulations, the shift was computed by aligning a simulated XANES spectrum of graphite with a measured XANES spectrum of highly oriented pyrolytic graphite. For the O 1*s* simulations, the shift was dictated by aligning the composite GO spectrum and the experimental spectra. As one can see from the results in Figure 3, the agreement between experiment and theory is excellent, particularly on the C 1*s* edge. The simulations shown here were calculated using the BJ functional, as with the water/graphene simulations, but we show, in Figure S2, a comparison of simulations, each of which uses one of the BJ, local-density approximation (LDA), or generalized gradient approximation (GGA) functionals. The structure was optimized using both spin-polarized LDA and spin-polarized GGA functionals. Regardless of which functional was used to optimize the structure, simulation of the TB-epoxide with the BJ functional group reproduces the strong resonance at 288.4 eV, and produces virtually no spectral weight at 285.2 eV. Additionally, the shape of the DOS above 290 eV is the right shape, albeit not quite broad enough. The agreement on the O 1*s* edge is not nearly as precise, but the majority of the spectral

DOI: 10.1021/acs.jpclett.5b00921
J. Phys. Chem. Lett. 2015, 6, 3163−3169

weight is nevertheless close to feature *d* at 534.9 eV. This is much better than any of the graphene/ice calculations achieved.

Compared to typical 1,2-epoxide functional groups, TB-epoxide is unstable. Table 2 lists the theoretical enthalpies of formation for graphene and several common graphene oxide moieties. The calculation procedure is outlined in the Supporting Information. Comparing the theoretical energy of formation per bond, TB-epoxide is more unstable than all of the other structures, except notably buckled graphene. (The buckled graphene cell was simply the TB-epoxide cell with the oxygen atoms removed.) This is why the changes to the electronic structure are reversible: Once the temperature is high enough for the externally induced strain on the lightly oxidized zones to relax, the third bond is broken on the top and bottom, and the room temperature-stable 1,2-epoxides form once more. This strain-dependent third C−O bond is ultimately the reason for the temperature-dependent elimination of the π^* feature at 285.2 eV. As we have shown previously, residual π-conjugated networks can still be found even on strongly oxidized graphene.[30] Strain-induced TB-epoxide makes the functionalization of the graphene lattice much more complete, thus destroying any residual π-conjugated pathways.

Table 2. Energy of Formations for Accepted Structures, As Compared to TB-Epoxide[a]

sample	overall C:O ratio	functional group present	ΔH° [eV/bond]	$\Delta H^\circ_x - \Delta H^\circ_{\text{graphene}}$ [eV/bond]
graphene	-	-	−1.254	0.000
SGO1	2:1	epoxide	−1.279	−0.025
SGO2	4:1	epoxide	−1.256	−0.002
SGO3	8:3	epoxide, hydroxyl, water	−1.377	−0.123
TB-epoxide	4:1	TB-epoxide	−1.142	0.112
buckled graphene	-	-	−1.117	0.137

[a]The structures of SGO1, SGO2, and SGO3 were originally published in ref 30.

In summary, we have found that, upon cooling four differently prepared samples of GO to 120 K, a pronounced change in the C and O unoccupied pDOS occurs. This low temperature state has no remaining π-conjugated states, unlike the high temperature state of GO. Between 120 K and room temperature, the two states can seemingly coexist. Similarities between our O 1*s* XANES spectra and spectra of amorphous solid water suggest that water intercalated between the GO sheets does not directly cause the observed change in the electronic structure. DFT simulations have instead shown that a new functional group, with a single O atom bonded to the 1,3,5 carbon sites, is responsible for this change in the electronic structure. However, the creation of this functional group, which we have called TB-epoxide, is only possible because of temperature-induced buckling of the lightly oxidized graphene zones, which is in turn the result of inhibited growth of the lightly oxidized zones due to the high negative thermal expansion coefficient exhibited by graphene. This change is entirely reversible, albeit with a significant hysteresis curve that results from the aforementioned metastability of the HT and LT states in the temperature region between room temperature and 120 K.

Although we observed the pronounced, reversible changes to the electronic structure of GO as a function of temperature, the root cause of the effect appears to be strain. As such, it may be possible to affect similar changes using externally applied stress. Applying compressive stress would have the effect of producing TB-epoxide, and thus removing the π-conjugated network. However, it is clear from the room temperature XANES spectra of all samples presented here, as well as many of the XANES spectra of GO presented in the literature, that spectral weight at 288.4 eV is a strong, and standard, feature. The origins of this feature have been discussed extensively.[35,36] If a significant portion of this spectral weight is, indeed, TB-epoxide in areas where buckling is already extensive, then applying tensile stress may help to rebuild the π-conjugated network. Much like pristine graphene, the electronic structure of GO can be affected by strain, but perhaps to an even greater degree.

EXPERIMENTAL SECTION

All C 1*s* XANES spectra were measured at the Spherical Grating Monochromator (SGM) beamline at the Canadian Light Source.[16] The exit slit to the monochromator was set to 25 μm, which gives the incident light an energy resolution better than 0.1 eV. The spectra were measured in both total electron yield mode and total fluorescence yield mode. The incident light linearly polarized, and the electric field component of the incoming light laid in the plane of incidence (p-polarization). All C and O 1*s* XANES spectra were measured with the incoming radiation striking at an angle of incidence of 30° from the normal of the sample. The temperature was lowered by pumping liquid nitrogen through the sample arm; the temperature was controlled via a heater located near the end of the sample arm.

For normalization, the O 1*s* and C 1*s* spectra were treated differently. For the O 1*s* spectra, the measured spectra were normalized to a signal generated simultaneously in a highly transparent gold mesh upstream of the sample; this gold mesh current is necessary and sufficient to quantify the incident flux. For the C 1*s* spectra, however, carbon contamination on all upstream optical components precludes the use of this elegant system. All C 1*s* spectra were instead normalized to the current generated in a photodiode.[37] This photodiode current spectrum was not taken simultaneously with the sample spectrum, but rather directly afterward.

ASSOCIATED CONTENT

Supporting Information

Details concerning the computation of the theoretical density of states, including the structures of the unit cells in CIF format. The Supporting Information is available free of charge on the ACS Publications website at DOI: 10.1021/acs.jpclett.5b00921.

AUTHOR INFORMATION

Corresponding Authors

*E-mail: adrian.hunt@usask.ca.
*E-mail: alex.moewes@usask.ca.

Present Addresses

[§]Department of Physics, North Carolina State University, 851 Main Campus Drive, Raleigh, North Carolina, 27606.
[∥]Institute of Materials Chemistry, Getreidemarkt 9, Vienna University of Technology, 1060 Vienna, Austria.

Notes

The authors declare no competing financial interest.

DOI: 10.1021/acs.jpclett.5b00921
J. Phys. Chem. Lett. 2015, 6, 3163−3169

■ ACKNOWLEDGMENTS

We acknowledge the efforts of Dmitriy Dikin, Sasha Stankovich, and his research group at Northwestern University at the Department of Chemistry, Northwestern University, USA. We acknowledge support by the Natural Sciences and Engineering Research Council of Canada (NSERC), the Canada Research Chair program, Canada Foundation for Innovation (CFI), and the Russian Foundation for Basic Research (Project 14-02-00006). The Canadian Light Source is supported by NSERC, the National Research Council (NRC) Canada, the Canadian Institutes of Health Research (CIHR), the Province of Saskatchewan, Western Economic Diversification Canada, and the University of Saskatchewan. We also acknowledge Compute Canada for the use of their computational resources, because the electronic structures of the reported structures, as well as many other failed candidates, were simulated on the Grex cluster at the University of Manitoba. The Grex cluster is part of Westgrid. Finally, we acknowledge Dr. Harald Ade, of North Carolina State University, that helped to get the manuscript into its final form.

■ REFERENCES

(1) Novoselov, K.; Geim, A.; Morozov, S.; Jiang, D.; Zhang, Y.; Dubonos, S.; Grigorieva, I.; Firsov, A. Electric field effect in atomically thin carbon films. *Science* **2004**, *306*, 666−669.

(2) Castro Neto, A. H.; Guinea, F.; Peres, N. M. R.; Novoselov, K. S.; Geim, A. K. The electronic properties of graphene. *Rev. Mod. Phys.* **2009**, *81*, 109−162.

(3) Huang, X.; Zeng, Z.; Fan, Z.; Liu, J.; Zhang, H. Graphene-Based Electrodes. *Adv. Mater.* **2012**, *24*, 5979−6004.

(4) Chang, H.; Wu, H. Graphene-based nanomaterials: synthesis, properties, and optical and optoelectronic applications. *Adv. Funct. Mater.* **2013**, *23*, 1984−1997.

(5) Kucinskis, G.; Bajars, G.; Kleperis, J. Graphene in lithium ion battery cathode materials: A review. *J. Power Sources* **2013**, *240*, 66−79.

(6) Stankovich, S.; Dikin, D. A.; Dommett, G. H. B.; Kohlhaas, K. M.; Zimney, E. J.; Stach, E. A.; Piner, R. D.; Nguyen, S. T.; Ruoff, R. S. Graphene-based composite materials. *Nature* **2006**, *442*, 282−286.

(7) Young, R. J.; Kinloch, I. A.; Gong, L.; Novoselov, K. S. The mechanics of graphene nanocomposites: A review. *Compos. Sci. Technol.* **2012**, *72*, 1459−1476.

(8) Hunt, A.; Dikin, D. A.; Kurmaev, E. Z.; Boyko, T. D.; Bazylewski, P.; Chang, G. S.; Moewes, A. Epoxide speciation and functional group distribution in graphene oxide paper-like materials. *Adv. Funct. Mater.* **2012**, *22*, 3950−3957.

(9) Zhu, Y.; James, D. K.; Tour, J. M. New routes to graphene, graphene oxide and their related applications. *Adv. Mater.* **2012**, *24*, 4924−4955.

(10) Mao, H. Y.; Lu, Y. H.; Lin, J. D.; Zhong, S.; Wee, A. T. S.; Chen, W. Manipulating the electronic and chemical properties of graphene via molecular functionalization. *Prog. Surf. Sci.* **2013**, *88*, 132−159.

(11) Su, Y.; Wei, H.; Gao, R.; Yang, Z.; Zhang, J.; Zhong, Z.; Zhang, Y. Exceptional negative thermal expansion and viscoelastic properties of graphene oxide paper. *Carbon* **2012**, *50*, 2804−2809.

(12) Huang, X.; Zhi, C.; Jiang, P.; Golberg, D.; Bando, Y.; Tanaka, T. Temperature-dependent electrical property transition of graphene oxide paper. *Nanotechnology* **2012**, *23*, 455705.

(13) Hauptmann, J. R.; Li, T.; Petersen, S.; Nygard, J.; Hedegard, P.; Bjornholm, T.; Laursen, B. W.; Norgaard, K. Electrical annealing and temperature dependent transversal conduction in multilayer reduced graphene oxide films for solid-state molecular devices. *Phys. Chem. Chem. Phys.* **2012**, *14*, 14277−14281.

(14) Dikin, D. A.; Stankovich, S.; Zimney, E. J.; Piner, R. D.; Dommett, G. H. B.; Evmenenko, G.; Nguyen, S. T.; Ruoff, R. S. Preparation and characterization of graphene oxide paper. *Nature* **2007**, *448*, 457−460.

(15) Stankovich, S.; Dikin, D. A.; Compton, O. C.; Dommett, G. H. B.; Ruoff, R. S.; Nguyen, S. T. Systematic post-assembly modification of graphene oxide paper with primary alkylamines. *Chem. Mater.* **2010**, *22*, 4153−4157.

(16) Regier, T.; Krochak, J.; Sham, T.; Hu, Y.; Thompson, J.; Blyth, R. Performance and capabilities of the Canadian Dragon: The SGM beamline at the Canadian Light Source. *Nucl. Instrum. Methods Phys. Res., Sect. A* **2007**, *582*, 93−95.

(17) Lee, V.; Dennis, R. V.; Jaye, C.; Wang, X.; Fischer, D. A.; Cartwright, A. N.; Banerjee, S. In situ near-edge x-ray absorption fine structure spectroscopy investigation of the thermal defunctionalization of graphene oxide. *J. Vac. Sci. Technol. B* **2012**, *30*, 061206.

(18) Nair, R. R.; Wu, H. A.; Jayaram, P. N.; Grigorieva, I. V.; Geim, A. K. Unimpeded permeation of water through helium-leak-tight graphene-based membranes. *Science* **2012**, *335*, 442−444.

(19) Boukhvalov, D. W.; Katsnelson, M. I.; Son, Y.-W. Origin of anomalous water permeation through graphene oxide membrane. *Nano Lett.* **2013**, *13*, 3930−3935.

(20) Acik, M.; Mattevi, C.; Gong, C.; Lee, G.; Cho, K.; Chhowalla, M.; Chabal, Y. J. The role of intercalated water in multilayered graphene oxide. *ACS Nano* **2010**, *4*, 5861−5868.

(21) Eigler, S.; Dotzer, C.; Hirsch, A.; Enzelberger, M.; Mueller, P. Formation and Decomposition of CO2 Intercalated Graphene Oxide. *Chem. Mater.* **2012**, *24*, 1276−1282.

(22) Kim, S.; Zhou, S.; Hu, Y.; Acik, M.; Chabal, Y. J.; Berger, C.; de Heer, W.; Bongiorno, A.; Riedo, E. Room-temperature metastability of multilayer graphene oxide films. *Nat. Mater.* **2012**, *11*, 544−549.

(23) Laffon, C.; Lacombe, S.; Bournel, F.; Parent, P. Radiation effects in water ice: A near-edge X-ray absorption fine structure study. *J. Chem. Phys.* **2006**, *125*, 204714.

(24) Marcotte, G.; Ayotte, P.; Bendounan, A.; Sirotti, F.; Laffon, C.; Parent, P. Dissociative adsorption of nitric acid at the surface of amorphous solid water revealed by x-ray absorption spectroscopy. *J. Phys. Chem. Lett.* **2013**, *4*, 2643−2648.

(25) Cavalleri, M.; Ogasawara, H.; Pettersson, L.; Nilsson, A. The interpretation of X-ray absorption spectra of water and ice. *Chem. Phys. Lett.* **2002**, *364*, 363−370.

(26) Gun'ko, V.; Turov, V.; Bogatyrev, V.; Zarko, V.; Leboda, R.; Goncharuk, E.; Novza, A.; Turov, A.; Chuiko, A. Unusual properties of water at hydrophilic/hydrophobic interfaces. *Adv. Colloid Interface Sci.* **2005**, *118*, 125−172.

(27) Angell, C. Liquid fragility and the glass transition in water and aqueous solutions. *Chem. Rev.* **2002**, *102*, 2627−2649.

(28) Blaha, P.; Schwarz, K.; Madsen, G. K. H.; Kvasnicka, D.; Luitz, J. *WIEN2k, An Augmented Plane Wave + Local Orbitals Program for Calculating Crystal Properties*; Karlheinz Schwarz, Technische Universitat Wien: Wien, Austria, 2001.

(29) Tran, F.; Blaha, P. Accurate band gaps of semiconductors and insulators with a semilocal exchange-correlation potential. *Phys. Rev. Lett.* **2009**, *102*, 226401.

(30) Hunt, A.; Kurmaev, E. Z.; Moewes, A. A re-evaluation of how functional groups modify the electronic structure of graphene oxide. *Adv. Mater.* **2014**, *26*, 4870−4874.

(31) Momma, K.; Izumi, F. VESTA 3 for three-dimensional visualization of crystal, volumetric and morphology data. *J. Appl. Crystallogr.* **2011**, *44*, 1272−1276.

(32) Bao, W.; Myhro, K.; Zhao, Z.; Chen, Z.; Jang, W.; Jing, L.; Miao, F.; Zhang, H.; Dames, C.; Lau, C. N. In situ observation of electrostatic and thermal manipulation of suspended graphene membranes. *Nano Lett.* **2012**, *12*, 5470−5474.

(33) Yoon, D.; Son, Y.-W.; Cheong, H. Negative thermal expansion coefficient of graphene measured by raman spectroscopy. *Nano Lett.* **2011**, *11*, 3227−3231.

(34) Zhu, J.; Andres, C. M.; Xu, J.; Ramamoorthy, A.; Tsotsis, T.; Kotov, N. A. Pseudonegative thermal expansion and the state of water in graphene oxide layered assemblies. *ACS Nano* **2012**, *6*, 8357−8365.

(35) Jeong, H.-K.; Noh, H.-J.; Kim, J.-Y.; Colakerol, L.; Glans, P.-A.; Jin, M.; Smith, K.; Lee, Y. Comment on "Near-edge x-ray absorption

DOI: 10.1021/acs.jpclett.5b00921
J. Phys. Chem. Lett. 2015, 6, 3163−3169

fine-structure investigation of graphene. *Phys. Rev. Lett.* **2009**, *102*, 099701.
(36) Pacile, D.; Papagno, M.; Rodriguez, A. F.; Grioni, M.; Papagno, L.; et al. Near-edge x-ray absorption fine-structure investigation of graphene. *Phys. Rev. Lett.* **2008**, *101*, 066806.
(37) Watts, B.; Thomsen, L.; Dastoor, P. Methods in carbon K-edge NEXAFS: Experiment and analysis. *J. Electron Spectrosc. Relat. Phenom.* **2006**, *151*, 105−120.

DOI: 10.1021/acs.jpclett.5b00921
J. Phys. Chem. Lett. 2015, 6, 3163−3169